

IET TRANSPORTATION SERIES 16

ICT for Electric Vehicle Integration with the Smart Grid

Other related titles:

- Volume 1 **Clean Mobility and Intelligent Transport Systems** M. Fiorini and J.-C. Lin (Editors)
- Volume 2 **Energy Systems for Electric and Hybrid Vehicles** K.T. Chau (Editor)
- Volume 5 **Sliding Mode Control of Vehicle Dynamics** A. Ferrara (Editor)
- Volume 6 **Low Carbon Mobility for Future Cities: Principles and applications** H. Dia (Editor)
- Volume 7 **Evaluation of Intelligent Road Transportation Systems: Methods and results** M. Lu (Editor)
- Volume 8 **Road Pricing: Technologies, economics and acceptability** J. Walker (Editor)
- Volume 9 **Autonomous Decentralized Systems and Their Applications in Transport and Infrastructure** K. Mori (Editor)
- Volume 11 **Navigation and Control of Autonomous Marine Vehicles** S. Sharma and B. Subudhi (Editors)
- Volume 12 **EMC and Functional Safety of Automotive Electronics** K. Borgeest
- Volume 25 **Cooperative Intelligent Transport Systems: Towards high-level automated driving** M. Lu (Editor)
- Volume 38 **The Electric Car** M.H. Westbrook
- Volume 45 **Propulsion Systems for Hybrid Vehicles** J. Miller
- Volume 79 **Vehicle-to-Grid: Linking electric vehicles to the smart grid** J. Lu and J. Hossain (Editors)

ICT for Electric Vehicle Integration with the Smart Grid

Edited by
Nand Kishor and Jesús Fraile-Ardanuy

The Institution of Engineering and Technology

Published by The Institution of Engineering and Technology, London, United Kingdom

The Institution of Engineering and Technology is registered as a Charity in England & Wales (no. 211014) and Scotland (no. SC038698).

© The Institution of Engineering and Technology 2020

First published 2019

This publication is copyright under the Berne Convention and the Universal Copyright Convention. All rights reserved. Apart from any fair dealing for the purposes of research or private study, or criticism or review, as permitted under the Copyright, Designs and Patents Act 1988, this publication may be reproduced, stored or transmitted, in any form or by any means, only with the prior permission in writing of the publishers, or in the case of reprographic reproduction in accordance with the terms of licences issued by the Copyright Licensing Agency. Enquiries concerning reproduction outside those terms should be sent to the publisher at the undermentioned address:

The Institution of Engineering and Technology
Michael Faraday House
Six Hills Way, Stevenage
Herts, SG1 2AY, United Kingdom

www.theiet.org

While the authors and publisher believe that the information and guidance given in this work are correct, all parties must rely upon their own skill and judgement when making use of them. Neither the authors nor publisher assumes any liability to anyone for any loss or damage caused by any error or omission in the work, whether such an error or omission is the result of negligence or any other cause. Any and all such liability is disclaimed.

The moral rights of the authors to be identified as authors of this work have been asserted by them in accordance with the Copyright, Designs and Patents Act 1988.

British Library Cataloguing in Publication Data

A catalogue record for this product is available from the British Library

ISBN 978-1-78561-762-1 (hardback)

ISBN 978-1-78561-763-8 (PDF)

Typeset in India by MPS Limited

Printed in the UK by CPI Group (UK) Ltd, Croydon

Contents

Preface	xiii
1 Advanced mobility communication	1
<i>Jorge Alfonso Kurano, David Jiménez Bermejo, Jesús Fraile-Ardanuy, Sandra Castaño, Julia Merino and Roberto Alvaro-Hermana</i>	
1.1 Introduction	1
1.2 Background	4
1.2.1 Cooperative ITS regulatory framework	4
1.2.2 State on cooperative ITS standardisation	10
1.2.3 Cooperative ITS developments and initiatives	10
1.2.4 3GPP initiatives	11
1.2.5 LTE-V and CV2X	15
1.3 Target services	18
1.4 Cooperative ITS current state	19
1.4.1 Standardisation in vehicular communications	19
1.4.2 List of related standards for cooperative ITS	30
1.5 5G and future mobility	32
1.6 Conclusions	33
References	34
Related standards	35
2 Grid integration and management of EVs through machine-to-machine communication	39
<i>Sayidul Morsalin, Khizir Mahmud, B.T. Phung and Jayashri Ravishankar</i>	
List of abbreviations	39
2.1 Introduction	41
2.2 M2M in distributed energy management systems	42
2.3 M2M communication for EVs	47
2.3.1 M2M communication architecture (3GPP)	48
2.4 Electric vehicle data logging systems	49
2.4.1 Data logging system	49
2.4.2 Hardware description	50
2.4.3 DLS operation	50

2.5	Scalability of electric vehicles	52
2.5.1	Radio resource and IP connection of LTE	53
2.5.2	Radio access of M2M	54
2.5.3	LTE user-plane protocol	55
2.5.4	Analytical model	56
2.5.5	Simulation and performance evaluation	59
2.6	M2M communication with scheduling	60
2.6.1	LTE scheduling	61
2.6.2	LTE popular scheduling algorithms	62
2.6.3	Performance evaluation	63
2.7	Conclusion	65
	References	65
3	Electrical vehicles charging and discharging scheduling for the cloud-based energy management service	69
	<i>Yu-Wen Chen</i>	
	List of abbreviation	69
3.1	Introduction	70
3.2	Cloud computing	71
3.3	Cloud-based energy management service	73
3.3.1	Framework and utilized data	74
3.3.2	Procedure	76
3.4	Electrical vehicles for the cloud-based energy management service	77
3.5	Scheduling results discussion	80
3.6	Conclusion	83
	References	84
4	Multi-criteria optimization of electric vehicle fleet charging and discharging schedule for secondary frequency control	87
	<i>Aleksandar Janjić and Lazar Z. Velimirović</i>	
	List of abbreviations	87
	Nomenclature	88
4.1	Introduction	89
4.1.1	Motivation	89
4.1.2	Literature review	90
4.1.3	Contribution	92
4.1.4	Chapter structure	92
4.2	Optimization problem	93
4.2.1	Frequency regulation	93
4.2.2	Business model	94
4.2.3	ICT architecture	95
4.2.4	Optimization objectives	96

4.3	Multi-objective optimization	100
4.3.1	Fuzzy multi-criteria decision-making	101
4.3.2	MAUT	102
4.4	Case studies	103
4.4.1	Belman–Zadeh approach	103
4.4.2	MAUT methodology	103
4.5	Conclusion	105
	Acknowledgments	107
	References	107
5	Power-demand management in a smart grid using electric vehicles	113
	<i>Khizir Mahmud, Mohammad Sohrab Hasan Nizami, Jayashri Ravishankar and M.J. Hossain</i>	
	List of abbreviations	114
5.1	Introduction	114
5.2	Power-demand management for single customer: Energy-resource-management technique	117
5.2.1	Load-management algorithm	118
5.2.2	EV charge management	121
5.2.3	Case studies	123
5.2.4	Comparison with an artificial neural network technique	125
5.3	Power-demand management for single customer: Load-management technique	126
5.3.1	HEMS model	126
5.3.2	Scheduling model	127
5.3.3	Case study	130
5.4	Power-demand management for multiple customers	133
5.4.1	General overview	133
5.4.2	Aggregated EV and power-demand management algorithm	134
5.4.3	Case studies	138
5.5	Conclusion	140
	References	140
6	Energy management of a small-size electric energy system with electric vehicles, flexible demands, and renewable generating units	145
	<i>Luis Baringo</i>	
6.1	Introduction	145
6.2	Notation	147
6.2.1	Indices	147
6.2.2	Sets	147
6.2.3	Parameters	147
6.2.4	Optimization variables	148

6.3	Modeling of electric vehicles	148
6.3.1	Individual modeling	148
6.3.2	EV aggregator	152
6.4	Deterministic energy-management problem	156
6.4.1	Objective function	156
6.4.2	Power balance constraints	156
6.4.3	Network constraints	157
6.4.4	Electric vehicle constraints	157
6.4.5	Demand constraints	157
6.4.6	Renewable production constraints	158
6.4.7	Formulation	158
6.5	Uncertainty characterization	161
6.6	Stochastic energy-management problem	162
6.7	Summary and conclusions	165
6.8	GAMS codes	165
6.8.1	Illustrative example 6.1	165
6.8.2	Illustrative example 6.2	167
6.8.3	Illustrative example 6.3	169
6.8.4	Illustrative example 6.5	172
	References	176
7	Peer-to-peer energy market between electric vehicles	177
	<i>Roberto Alvaro-Hermana, Julia Merino, Jesús Fraile-Ardanuy, Sandra Castaño-Solis and David Jiménez</i>	
	List of abbreviations	177
	List of parameters and variables	178
7.1	Introduction	179
7.2	Activity-based model	181
7.3	Consumption model and drivers classification	184
7.3.1	Consumption model	184
7.3.2	Drivers classification	185
7.4	Intermediate charging process optimization	188
7.5	Peer-to-peer trading system	193
7.5.1	Determining the final price for the P2P trading system each TAZ and each time period	194
7.5.2	Quadratic programming formulation	197
7.5.3	Proposed algorithm for solving the P2P market trading	198
7.6	Results of the P2P energy market	198
7.6.1	Individual analysis of vehicles from sets A and B	198
7.6.2	Electricity price analysis at TAZ level	201
7.7	Long-term peer-to-peer energy market	202
7.8	Conclusions	204
	References	205

8 Dispatch of vehicle-to-grid battery storage using an analytic hierarchy process	209
<i>Lu Wang, Suleiman Sharkh and Andy Chipperfield</i>	
8.1 Introduction	209
8.2 Battery characteristics	210
8.3 Dispatch strategy of electric vehicle battery storage	211
8.3.1 AHP hierarchy process	212
8.3.2 Determination of the dispatch action	215
8.4 Simulation test	222
8.5 Sensitivity analysis	228
8.6 Conclusions	235
References	236
9 Electric vehicles as distributed energy storage for local energy management	239
<i>Ricardo Morales, Jesús Fraile-Ardanuy, Álvaro Gutiérrez, David Jiménez, Benito Artaloytia, Roberto Álvaro-Hermana, Julia Merino and Sandra Castaño-Solis</i>	
9.1 Introduction	239
9.2 System description	240
9.2.1 Building PV generation and electricity consumption	240
9.2.2 Grid electricity price	243
9.2.3 Mobility information	243
9.3 Optimization modelling	248
9.4 Scenarios and results	250
9.5 Conclusions	264
References	265
10 Contribution of electric vehicles to power system ancillary services beyond distributed energy storage	267
<i>Sergio Martínez, Hugo Mendonça, Rosa M. de Castro and Danny Ochoa</i>	
List of abbreviations	267
10.1 Introduction	268
10.2 Contribution of electric vehicles to the power system frequency control	269
10.2.1 Theoretical background	270
10.2.2 Case study	270
10.3 Contribution of electric vehicles to voltage control	275
10.3.1 Theoretical background	275
10.3.2 Unbalanced three-phase power flow	276
10.3.3 Contribution of electric vehicles to voltage control	277
10.3.4 Case study	278

10.4 Conclusion	283
Acknowledgements	283
References	284
11 Electric vehicles for renewable energy integration in isolated power systems	287
<i>Yaofang Wang, Sandra Castaño-Solis, Jesús Fraile-Ardanuy, David Jiménez, Benito Artaloytia, Roberto Álvaro-Hermana and Julia Merino</i>	
11.1 Introduction	287
11.2 El Hierro's electrical system description	289
11.3 Data description	291
11.3.1 Electric power system data	291
11.3.2 Mobility data	294
11.4 Optimization algorithm for night charging	296
11.5 Scenarios	297
11.5.1 Scenario 1. Base scenario. No VE-No PHEP	297
11.5.2 Scenario 2. Base scenario+VEs-No PHEP	299
11.5.3 Scenario 3. Base scenario+VEs-PHES	302
11.6 Conclusion	314
References	315
12 A solar- and wind-powered charging station for electric buses based on a backup batteries concept	319
<i>Jakub Jurasz and Bartłomiej Ciapala</i>	
12.1 Introduction	319
12.1.1 Related works	320
12.2 Methods and data	322
12.2.1 Methods and problem formulation	322
12.2.2 Input data	323
12.3 Discussion and results	326
12.3.1 Self-sufficiency and reliability of supply	326
12.3.2 Economic analysis	328
12.3.3 Environmental impact	331
12.3.4 Impact on the grid	332
12.3.5 Future works	334
12.4 Conclusion	334
References	335
13 Deploying stochastic coordination of electric vehicles for V2G services with wind	339
<i>Sulabh Sachan and Nand Kishor</i>	
Notation	339
13.1 Introduction	340

13.2	Test system	342
13.3	Probabilistic model of wind power	342
13.4	Stochastic load modeling of EV	344
	13.4.1 Stochastic adaptive fuzzy model of EVs	346
	13.4.2 Charging level and type of EVs	348
	13.4.3 Initial <i>SOC</i> and EVs load profile	348
13.5	Financial and operational modeling	349
	13.5.1 Real-time pricing policy	349
	13.5.2 Degradation cost of EVs battery	349
	13.5.3 Frequency regulation	350
	13.5.4 Spinning reserves	350
13.6	Formulation of charging/discharging strategy	350
	13.6.1 Charging/discharging energy of EVs	351
	13.6.2 Optimizing strategy and function	352
	13.6.3 ESPSO	353
13.7	Case studies and discussion	354
	13.7.1 Comparison of load profiles of EVs on different modeling schemes	354
	13.7.2 Impact of wind and EV penetration	354
13.8	Conclusion	358
	References	358
14	Optimal location and charging of electric vehicle with wind penetration	361
	<i>Sulabh Sachan and Nand Kishor</i>	
	Nomenclature	361
14.1	Introduction	363
14.2	Test system	365
14.3	Sensitivity analysis	366
	14.3.1 Node selection	368
	14.3.2 System operation algorithm	370
14.4	Stochastic modeling for EVs load demand	372
	14.4.1 Charging level and type of EVs analysis	373
	14.4.2 Stochastic fuzzy modeling	374
	14.4.3 Initial <i>SOC</i> and EVs load profile	375
14.5	Peak load shifting optimization	375
	14.5.1 EV charging optimization according to load curve	376
	14.5.2 EV charging optimization according to real-time price	377
	14.5.3 EV charging optimization according to wind power and RTP	378
	14.5.4 Charging/discharging shifting	378
14.6	Conclusion	382
	References	382

15 Optimal coordination of vehicle-to-grid batteries and renewable generators in a distribution system	385
<i>Lu Wang, Suleiman Sharkh and Andy Chipperfield</i>	
15.1 Introduction	385
15.2 General description of the electricity network and agents	386
15.3 Formulation of DMOCOP	388
15.3.1 Objectives	388
15.3.2 The AHP	392
15.3.3 Constraints	393
15.4 A* optimal dispatch procedure	394
15.5 The application of A* search to optimal decentralized coordination of EVs and RGs in a distribution network	400
15.5.1 Stochastic modelling of uncertainties	400
15.5.2 Simulation results	406
15.6 Complexity discussion	412
15.7 Conclusion	415
References	416
Index	419

Preface

Smart power grid technologies pertain to the system wherein the energy resources, storage, information flow, feedback loop involve a complex decision-making in dynamic interconnected power system. Among the technologies, electric vehicles (EVs) have spurred new paradigms for smart grid operation. Recently, researchers and manufacturers in EV sector have much talked about the application of EVs in grid operation for its effective management.

EVs offer high energy efficiency and a cleaner mode of personal transportation. The EV is a new type of load being accommodated into power network. Its impact on power system will depend on its penetration level. A large-scale adoption of EVs will pose new challenges to system operators since their charging can cause technical problems, such as voltage limits violating or line congestion, mainly at the distribution level.

The fact that EV is a highly distributed electric energy storage device, its integration into the grid system gives an opportunity to support the system operation. It is possible to mitigate either partly or fully the negative impacts on integrating EVs in the grid, with maximization of positive impacts. Although EVs introduce new challenges on grid capacity, it may support the grid stability. There is a huge prospect of exploitation of EVs for smart grid applications.

Therefore, it is interesting to develop tools and strategies that allow tackling these or anticipating their consequences. In general, the so-called EV aggregators will try to maximise their benefits by allocating charging to the most favourable time periods. EVs in smart grid operation require a wide coverage with flexible and cost-effective communication networks. The communication, networking and information technologies will play a vital role in the development of smart grid by supporting two-way energy (charging & discharging of EVs) and information flow. This will enable efficient monitoring, control and optimization of power imbalance in the grid.

In general, the chapters in book contribute to address the EVs as a driving source for realizing the smart grid operation. The book includes chapters from multi-disciplinary research/industry communities, related to EVs charging schemes/technologies, and its associated communication, networking and information architectures, and ancillary services of EVs for power grid management.

Chapters 1–4 present the use of communication network/infrastructure including communication properties, cloud-based energy management service for V2F integration. Chapters 5–7 discuss power/energy management strategy applying

optimization models. Chapter 8 presents peer-to-peer energy market model. Chapters 9–11 contribute in the lines of EVs as storage application for grid management. Chapters 12–15 discuss on charging/discharging strategy of EVs with integration of renewable energy resources in the distribution grid.

AQ1

Nand Kishor and Jesús Fraile-Ardanuy
Editors

Prelims
Author Query

AQ1: Please check and confirm if “Chapters 12–16” can be changed to “Chapters 12–15” as there are only 15 chapters present in this book.

Chapter 9

Electric vehicles as distributed energy storage for local energy management

*Ricardo Morales¹, Jesús Fraile-Ardanuy²,
Álvaro Gutiérrez², David Jiménez², Benito Artaloytia²,
Roberto Álvaro-Hermana^{3,4}, Julia Merino⁵ and
Sandra Castaño-Solis⁶*

9.1 Introduction

Electric vehicles (EVs) are relatively new at a commercial scale and are currently dealing with issues like cost, anxiety range and charging capacity [1]; but, they offer enormous possibilities for reducing CO₂ and NO_x emissions and carbon footprint if they are integrated by means of renewable sources [2,3].

As the production cost of photovoltaic (PV) energy is closing to the retail prices [4], it is possible to make self-consumption installations profitable, reducing the amount of energy required from the utility grid and decreasing the total electricity cost. In order to achieve this objective, it is necessary to combine the PV generation with electricity storage and demand-response schemes [5–7].

In an office building with PV generation, some of these restrictions can be easily resolved. There is an alignment of working hours with the PV energy production, and there are two different situations that must be analysed. First, if PV generation exceeds the building energy demand during the day, this surplus energy must be stored in a battery and fed back into the building grid when the PV generation is lower than the building energy demand. Thus, PV coverage of energy demand (self-consumption) increases. Second, if PV generation is lower than the building energy demand during all time periods, it is still possible to save money, storing the energy in the batteries when the retail prices are low and powering it back into the building when the utility prices are at the highest value, optimizing

¹Fronius México SA, Puebla, Mexico

²ETSI Telecomunicación, Universidad Politécnica de Madrid, Madrid, Spain

³Orkestra – Basque Institute of Competitiveness, Bilbao, Vizcaya, Spain

⁴University of Deusto, Bilbao, Vizcaya, Spain

⁵TECNALIA, Parque Científico y Tecnológico de Bizkaia, Derio, Spain

⁶Escuela Técnica Superior de Ingeniería y Diseño Industrial (ETSIDI), Universidad Politécnica de Madrid, Madrid, Spain

the total electricity cost paid by the building manager. This second situation, where PV energy is the only one used to charge the vehicles, is used in this work.

Even though the Li-ion battery price has dropped significantly in recent years [8], this storage technology is still quite expensive and, in order to avoid overspending, this study proposes using EV's batteries as Battery Energy Storage System. One of the main disadvantages of this scheme is that the total available battery's capacity is variable, but it is dependent on the EV's mobility. In this chapter, an optimization model is developed to minimize the electricity cost purchased from the utility grid by the building manager. This optimization model takes into account several parameters: the availability of the EVs parked at the parking lot (that affects the available storage capacity, which varies at each time period, as EVs come and go along the day), the total energy consumption demanded by the building, the self-PV generation and, finally, the retail energy prices. With this information, the optimization algorithm determines how the EV batteries' charge/discharge of all parked vehicles should be managed to minimize the cost of electricity purchased from the grid.

The optimization system also considers several constraints: the amount of energy that should be stored in each battery at the end of the day, and the maximum energy that can be charged/discharged from these vehicles. We will apply this model to a real building consumption profile.

9.2 System description

9.2.1 Building PV generation and electricity consumption

The *Instituto de Energía Solar*-IES (Solar Energy Institute) is a research centre from Universidad Politécnica de Madrid founded in 1978 and specifically focuses on the fundamentals and practical application of PVs systems. Its headquarters are located at EscuelaTécnica Superior de Ingenieros de Telecomunicación Universidad Politécnica de Madrid (ETSIT-UPM), in Madrid (Spain), and it shares a common parking area with a total capacity of 29 parking decks, as is shown in Figure 9.1.

The total built area of IES is 875 m², distributed on three floors, containing several research laboratories, meeting rooms and offices for researchers. There are 13.1 kWp PV cells installed at IES headquarters, integrated into the roofs and the facades, which are shown in Figure 9.2. The PV panel tilt is $\theta_{tilt} = 26^\circ$ and it is oriented directly to the South ($\theta_{orientation} = 0^\circ$). This PV generation is monitored with an hour resolution, along with the total consumption of the building. These measurements are available online at <http://monitoring.robolabo.etsit.upm.es/etsit/monitoring.php?tab=ies>

Figure 9.3 shows the PV hourly energy generation (in kWh) and the total hourly electricity consumption of this building (in kWh) for three typical working weeks in March, April and May 2016. A blue dotted line represents PV generation, while electric demand is shown with a brown dotted line.

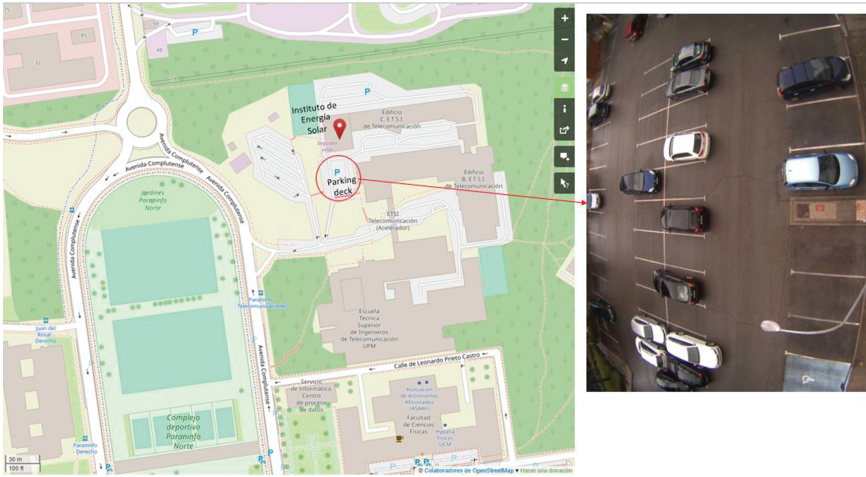


Figure 9.1 Instituto de Energía Solar (Solar Energy Institute) headquarters location with the parking decks highlighted



Figure 9.2 Instituto de Energía Solar (Solar Energy Institute) building

It is observed that, during this 3-month period, the average load demand is around 32 kWh and the peak electric consumption reaches almost 60 kWh, while the maximum PV generation was 8.8 kWh during this period (14%–67% of the peak demand). For that reason, there is not enough PV-generated energy to satisfy all energy load demand of this research centre.

An average week of IES PV hourly energy generation for each season of the year is shown in Figure 9.4. The highest solar production is obtained during spring and autumn seasons, when the outdoor temperature is cooler and the PV panel efficiency is increased. During the winter season, even though the outdoor

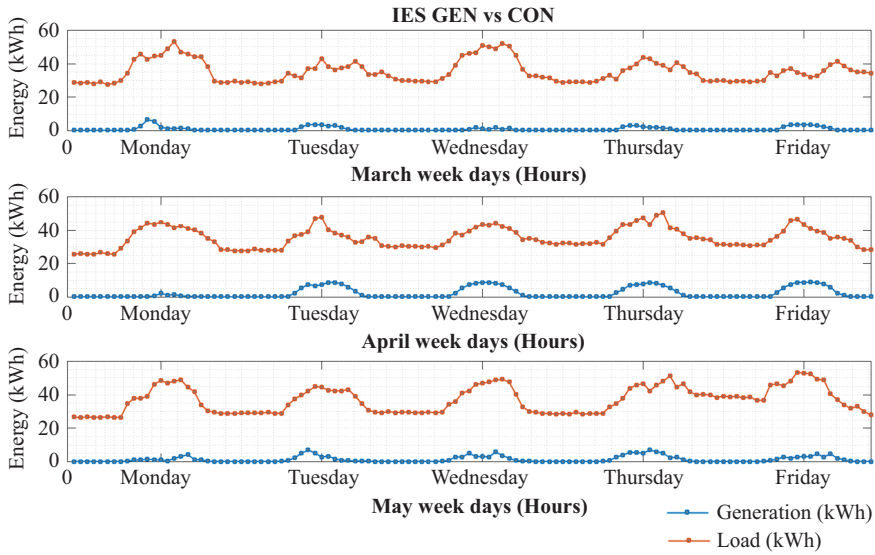


Figure 9.3 *IES PV generation (blue line) and electric consumption (brown line) during three different working weeks in March, April and May 2018*

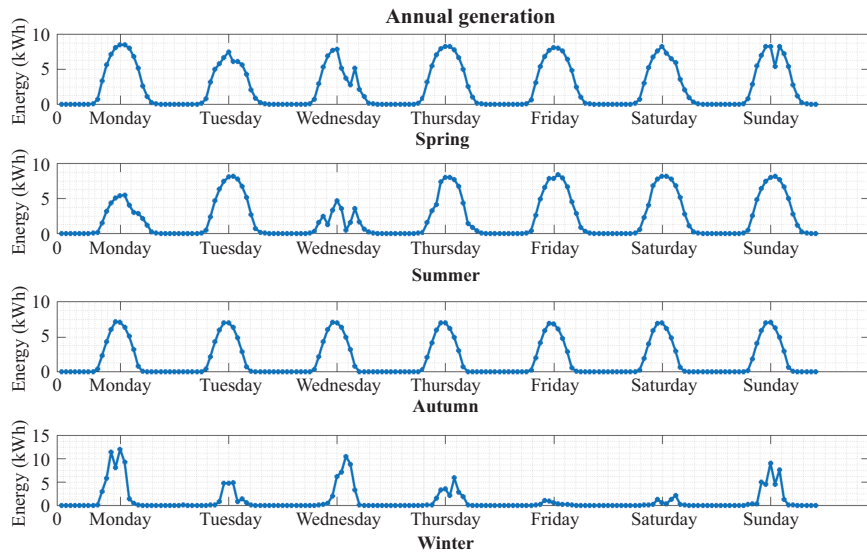


Figure 9.4 *IES PV hourly generation (blue line) during an average week in each season of the year*

temperature is lower and the panel efficiency is higher, the days are shorter, with less sunlight, and thus the PV generation is significantly reduced.

9.2.2 Grid electricity price

Currently, there are three different electric tariffs in Spain [9]: normal rate 2.0A (which is the default hourly tariff), night rate 2.0 DHA (which is a two periods hourly tariff, with cheaper prices during the night but more expensive prices during the day) and EV rate 2.0 DHS (which is a small variation of the previous 2.0 DHA, with even cheaper prices from 00:00 to 06:00 hours well suited for EVs).

The hourly prices of each of these tariffs are changing every day. Four different representative days, one for each season has been selected for this study. Figure 9.5 shows the three electric tariffs (2.0A, 2.0DHA and 2.0DHS) for these four representative days in spring, summer, autumn and winter.

9.2.3 Mobility information

In order to estimate the aggregated battery capacity available at each hour of the day, the first step was to analyse the parking occupation. With this information, it was possible to know how many vehicles were parked at IES along the day.

Once the parking occupation was calculated, the second step was to estimate the consumption of these vehicles and the energy required to reach the final destination at the end of the day. From this information, the total aggregated battery capacity available for the proposed building energy management was estimated.

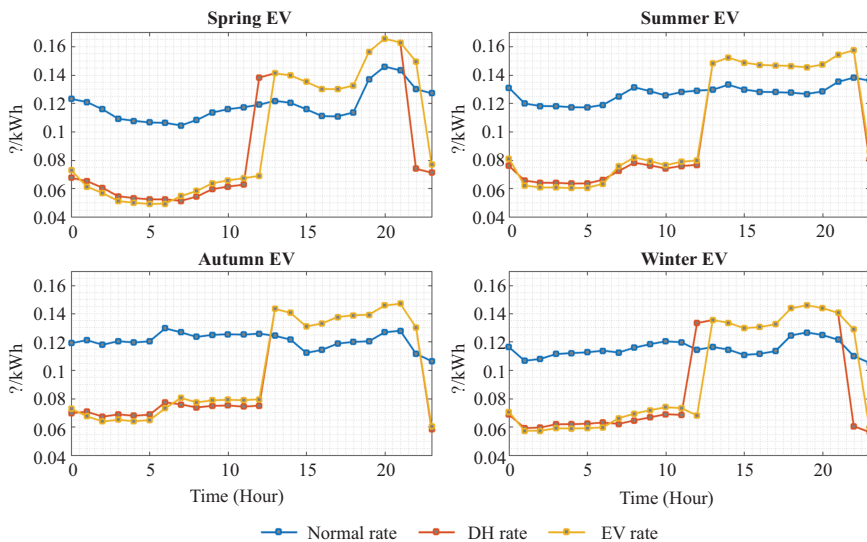


Figure 9.5 Hourly electric tariffs during different seasons

9.2.3.1 Parking occupation

Figure 9.6 shows IES’s EV parking deck with 29 places at different time periods. The first (top-left) image in this figure was taken at 10:00 a.m. on Saturday morning and it is observed that there were no vehicles parked at this moment. The second (bottom-left) image from this figure was taken at 8:00 a.m. on Wednesday morning and there were 12 different vehicles parked at this particular hour.

A camera was installed in the parking and the available free parking lots were detected using an artificial intelligence–based algorithm developed in Python and previously trained. The total number of vehicles and free spots are available in real time.

The parking was monitored during five consecutive working days (from Monday to Friday) for 3 months. With this information, an hourly occupancy matrix, such as the one shown in Figure 9.6 (right), was generated for each working day of the week.

In this work, an additional sixth-day scenario was defined to consider a constant static battery capacity. This effect will be simulated in our work, considering that 29 EV were parked all day long.

Figure 9.7 shows the six different hourly occupancy matrix, from Monday to Friday plus the previously defined sixth day. There are 24 different columns in each matrix representing different hours and there are 29 rows, representing each parking deck. Dark blue squares represent free decks, while light blue squares indicate that there is a vehicle parked in this position (defined by the specific row), at this particular time slot (defined by the specific column).

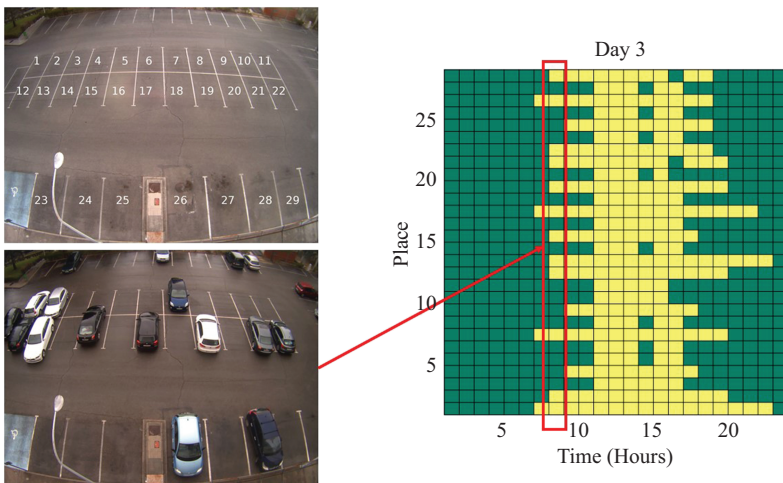


Figure 9.6 EV parking occupation

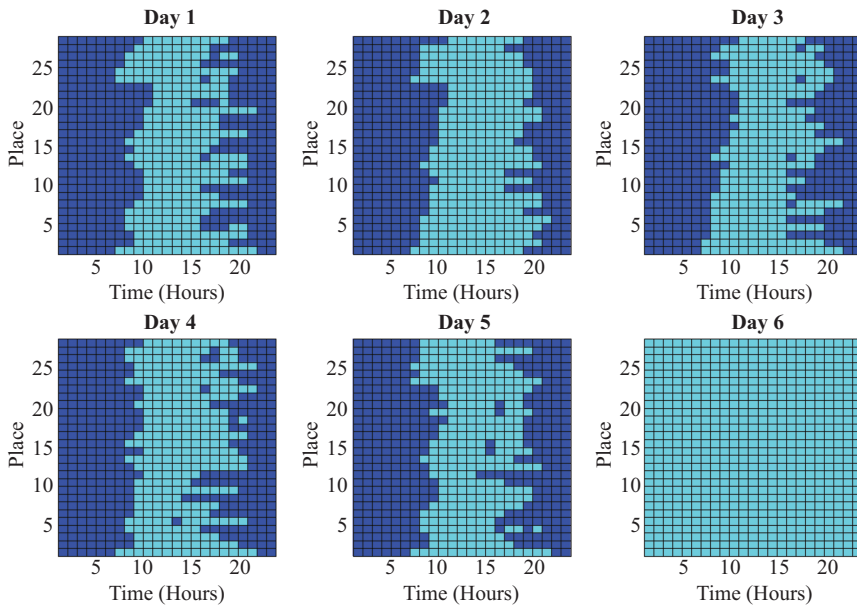


Figure 9.7 Occupation behaviour

9.2.3.2 Initial available capacity

For this research, it is assumed that all vehicles are electric and of the same model (a Nissan Leaf 2016, with a nominal capacity of 30 kWh [10]) and all these cars belong to the IES fleet.

Nissan Leaf has two different charging options, both located at a common charge port at the front of the car: a CHAdeMO inlet, which allows charging to 80% of the nominal battery capacity in 30–40 min (at 50 kW ac) and a conventional Type 2 socket, with a default 3.7 kW onboard charger, which allows charging to 100% of the capacity in 12–14 h (there are some Nissan Leaf models, SV and SL grades, with a 6.7 kW onboard charger available).

In this work, it is assumed that all vehicles can be charged and discharged with maximum power up to 3.7 kW. Additionally, it is also assumed that only 12% of the total capacity available (3.6 kWh) can be used to support the building power grid, in order to reduce battery degradation due to the over-cycling process.

A quantitative online mobility survey was carried out for IES workers to provide insightful information regarding their daily mobility behaviours and 30 employees answered this daily mobility survey. In Figure 9.8, the histogram of the daily average distance travelled by them and the location of the origin of their daily trips are presented. Analysing this figure, it is observed that most of the employees travel less than 30 km per day. The average daily distance is 26.95 km and the maximum distance is 90 km.

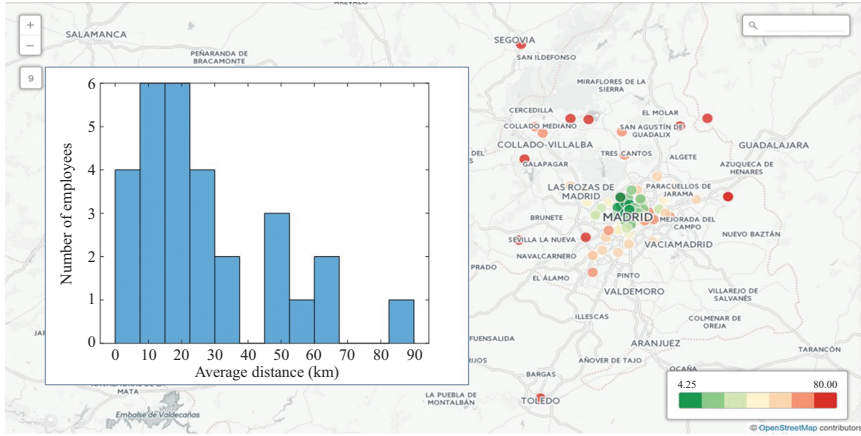


Figure 9.8 *Daily distance histogram (left) and the location of the origin of the daily trips (right)*

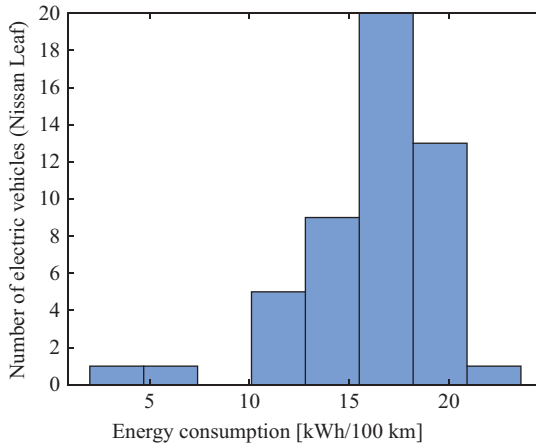


Figure 9.9 *Histogram of energy consumption of Nissan Leaf vehicle under real-life conditions*

The information about vehicle consumption is obtained from [11], which is a website where users update their fuel consumptions under real driving conditions. The histogram of the electric consumption of 50 different Nissan Leaf owners is presented in Figure 9.9. The average consumption is 16.02 kWh/100 km, with a minimum value of 3.26 kWh/100 km and a maximum value of 22.91 kWh/100 km.

In order to generate different consumptions for each EV, an initial average distance is randomly selected from Figure 9.8. This value is then multiplied by a randomly selected consumption sample extracted from the histogram presented in

Figure 9.9, providing a particular electric consumption value for each EV. All this procedure is highlighted in Figure 9.10. With this data, each particular EV has a slightly different consumption, providing some variability to the model.

Taking into account the mobility constraints of these vehicles during the day, and the available battery capacity of each vehicle in each time period, the aggregated total battery capacity available for the proposed building energy-management system is evaluated, as shown in Figure 9.11.

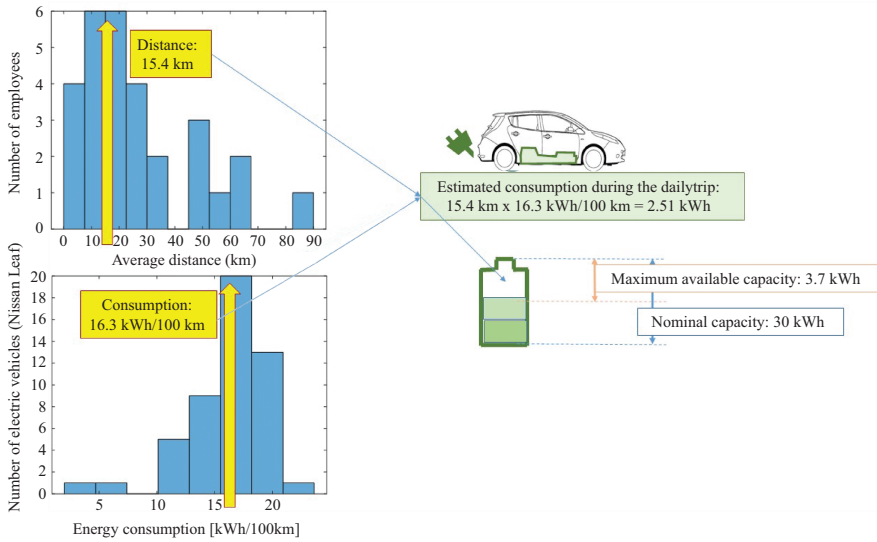


Figure 9.10 Initial battery capacity available per vehicle

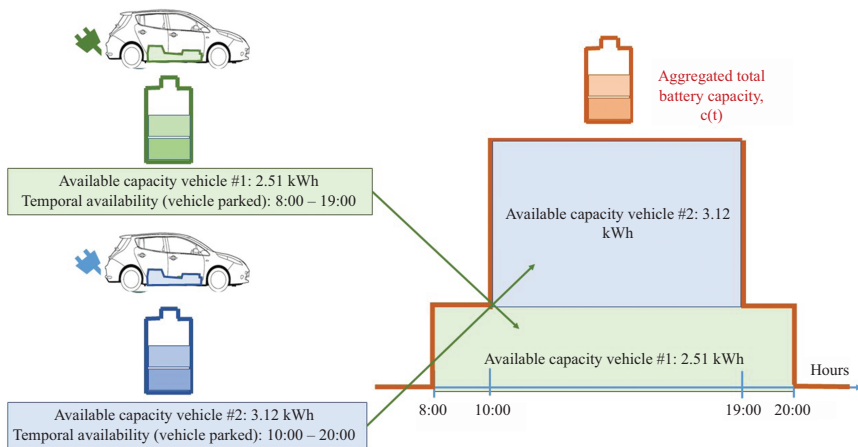


Figure 9.11 Aggregated battery capacity

9.3 Optimization modelling

The optimization problem formulation is defined in this section. Figure 9.12 and Table 9.1 present the main variables and parameters used in this model. The system equations are defined in (9.1)–(9.4).

Equation (9.1) describes the dynamic evolution of the aggregated battery capacity, which depends on the current number of vehicles parked at this period of time, their initial batteries’ state of charge and the energy injected/extracted from

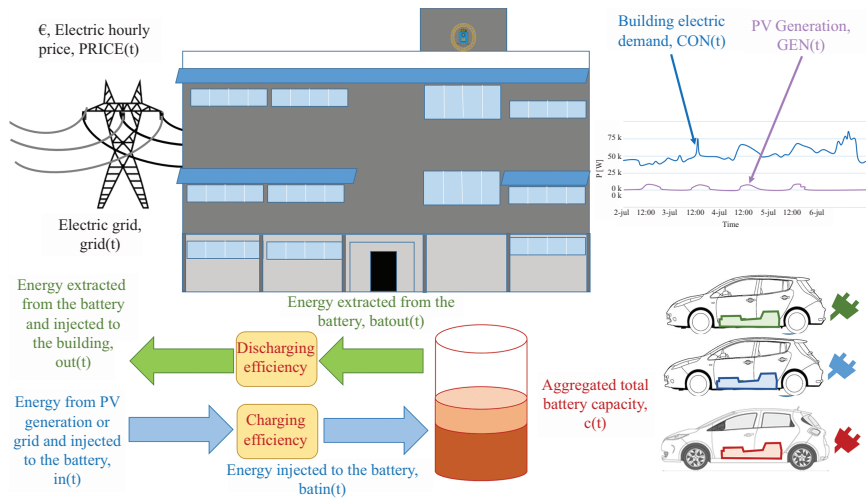


Figure 9.12 Optimization model description

Table 9.1 Variables and parameters from the optimization model

Symbol	Description	Length
$CON(t)$	IES Building electric consumption per hour	1×24
$GEN(t)$	IES Building PV generation per hour	1×24
$PRICE(t)$	Hourly electricity price	1×24
$grid(t)$	Energy extracted from the electric grid per hour	1×24
$c_{max}(t)$	Maximum aggregated battery capacity per hour	1×24
$in(t)$	Energy stored in the aggregated battery per hour	1×24
$out(t)$	Energy extracted from the aggregated battery per hour	1×24
$c(t)$	State of Charge (SOC) of the aggregated battery per hour	1×24
$Occupation(t)$	Number of vehicles parked per hour	1×24
c_{ini}	Initial capacity	1×1
P_{max}	Charging/Discharging nominal power	1×1

this aggregated battery. The parameter c_{ini} is the initial capacity of the aggregated battery. This parameter is zero on the first 5 days (from day 1 to day 5) because there are not EVs parked initially, but this value can change on day 6, when a static battery is assumed to be installed in the proposed system.

Equations (9.2) and (9.3) take into account the charging/discharging efficiency. Finally, (9.4) determines the energy directly extracted from the electric grid to cover the total demand of this system.

$$c(t) = \begin{cases} c(t-1) - \text{batout}(t) + \text{batin}(t) & \forall t > 1 \\ c_{ini} - \text{batout}(t) + \text{batin}(t) & t = 1 \end{cases} \quad (9.1)$$

$$\text{batin}(t) = \eta_{\text{charging}} \text{in}(t) \quad \forall t \quad (9.2)$$

$$\text{batout}(t) = \frac{\text{out}(t)}{\eta_{\text{discharging}}} \quad \forall t \quad (9.3)$$

$$\text{grid}(t) = \text{CON}(t) - \text{GEN}(t) - \text{out}(t) + \text{in}(t) \quad \forall t \quad (9.4)$$

The objective function to minimize is given by (9.5). This equation evaluates the daily energy cost bought to the electric grid, and the solution of this optimization problem will provide the lowest price to pay at the end of the day.

$$lc = \min \left[\sum_{t=1}^{24} \text{PRICE}(t) \cdot \text{grid}(t) \right] \quad (9.5)$$

Equations (9.1)–(9.5) must be subjected to the following constraints:

$$c(t) \leq c_{\max}(t) \quad \forall t \quad (9.6)$$

$$\text{out}(t) \leq P_{\max} \cdot \text{occupation}(t) \quad \forall t \quad (9.7)$$

$$\text{in}(t) \leq P_{\max} \cdot \text{occupation}(t) \quad \forall t \quad (9.8)$$

where (9.6) indicates that the current capacity of the aggregated battery, $c(t)$, must be lower than $c_{\max}(t)$, which is the maximum hourly available capacity. This upper limit is not constant and it will depend on the parking stop dynamics.

The variables, $c(t)$, $\text{out}(t)$ and $\text{in}(t)$ are always defined positive.

If all vehicles are parked during all day, this maximum capacity will be $3.7 \text{ kWh} \times 29 = 107 \text{ kWh}$ as it is shown in Figure 9.13 (day 6 blue line). In this figure, the maximum hourly available capacity per day is presented, according to the parking occupation shown in Figure 9.7. It is observed that $c_{\max}(t)$ is different during each hour and each day of the week.

The following two equations, (9.7) and (9.8), indicate that the energy that can be injected/extracted from this distributed storage system must be lower than the product of the number of available EVs parked at hour t , given by the variable $\text{Occupation}(t)$, and the maximum charging power, which is limited to 3.7 kW.

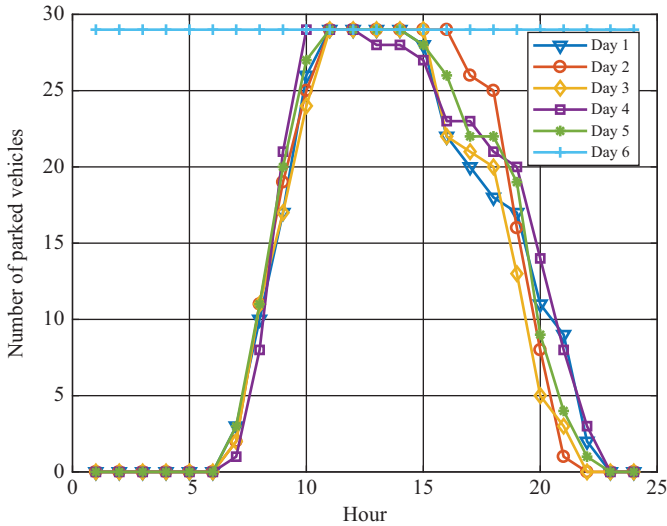


Figure 9.13 Aggregated battery capacity per day

9.4 Scenarios and results

Different scenarios were simulated over 3 months varying EVs parked occupancy, retail electricity price, PV generation and building consumption. These scenarios are defined in Table 9.2.

In Figure 9.14, the first scenario (Day 1) is analysed in detail. Vehicles start arriving at IES headquarters early in the morning (at 7:00 a.m.). Since the energy price is still very low during these hours of the day (denoted by a blue line in the figure), EVs begin to store energy in their batteries (as indicated by the green bars in this figure).

As IES workers continue arriving at their offices, the number of EV available in the parking lot increases (shown by the red line in Figure 9.14) and the optimization building-energy-management system (OBEMS) keeps charging their batteries until 11:00 a.m. At this time, all batteries are completely full and it is not possible to store more energy.

At 13:00 p.m., the EV tariff profile presents a sudden increment and the OBEMS extracts energy from the batteries and injects it into the building grid, which is represented by red bars in the figure, reducing almost to zero the energy purchased to the utility company (depicted by the black line in the figure) during 2 hours (from 14:00 to 16:00 p.m.).

There is a maximum value for the electricity price at 20:00 p.m. For that reason, the OBEMS starts to charge the remaining EVs at 18:00 p.m. and this stored energy is discharged later in the last three available hours (from 19:00 to 22:00 p.m.). Note that IES remains closed from 22:00 p.m. to 7:00 a.m.

Table 9.2 Scenarios under analysis

Season	EV Tariff		DH Tariff		Default Tariff		Occupation
Spring	Day 1	Figure 9.17(a)	Day 25	Figure 9.19(a)	Day 49	Figure 9.21(a)	Occupation 1
	Day 2		Day 26		Day 50		Occupation 2
	Day 3		Day 27		Day 51		Occupation 3
	Day 4		Day 28		Day 52		Occupation 4
	Day 5		Day 29		Day 53		Occupation 5
	Day 6		Day 30		Day 54		Constant Occup.
Summer	Day 7	Figure 9.17(b)	Day 31	Figure 9.19(b)	Day 55	Figure 9.21(b)	Occupation 1
	Day 8		Day 32		Day 56		Occupation 2
	Day 9		Day 33		Day 57		Occupation 3
	Day 10		Day 34		Day 58		Occupation 4
	Day 11		Day 35		Day 59		Occupation 5
	Day 12		Day 36		Day 60		Constant Occup.
Autumn	Day 13	Figure 9.18(a)	Day 37	Figure 9.20(a)	Day 61	Figure 9.22(a)	Occupation 1
	Day 14		Day 38		Day 62		Occupation 2
	Day 15		Day 39		Day 63		Occupation 3
	Day 16		Day 40		Day 64		Occupation 4
	Day 17		Day 41		Day 65		Occupation 5
	Day 18		Day 42		Day 66		Constant Occup.
Winter	Day 19	Figure 9.18(b)	Day 43	Figure 9.20(b)	Day 67	Figure 9.22(b)	Occupation 1
	Day 20		Day 44		Day 68		Occupation 2
	Day 21		Day 45		Day 69		Occupation 3
	Day 22		Day 46		Day 70		Occupation 4
	Day 23		Day 47		Day 71		Occupation 5
	Day 24		Day 48		Day 72		Constant Occup.

Figure 9.15 shows the charging/discharging profile from day 34, which represents an average summer day with DH tariff. It is observed that the EVs from early workers were recharged from 7:00 to 8:00 a.m. when the electricity price was the lowest. Then, entry of workers was not as staggered as during the previous scenario and for that reason, the batteries were fully charged at 11:00 a.m., taking advantage of the low electricity price at this particular hour. This energy was progressively discharged until 16:00 p.m. and, at the end of the day, the OBEMS determined to charge (at 20:00 p.m.) and discharge (at 21:00 p.m.) the stored energy, taking advantage of the maximum electricity price at 21:00 p.m. and significantly reducing the amount of energy purchased to the grid.

Figure 9.16 shows the charging/discharging profile from day 62, which represents an average autumn day with normal tariff. The charging/discharging profiles are similar to the previous figures, but in this particular scenario, the electricity price does not have two clearly differentiated periods.

Finally, Figure 9.17 presents the charging/discharging profile from day 72, which represents an average winter day with normal tariff and constant occupation (all vehicles are available during the whole day). These EVs are charged at the lowest electricity price (6:00) and the profile and discharging when the electricity price is the highest.

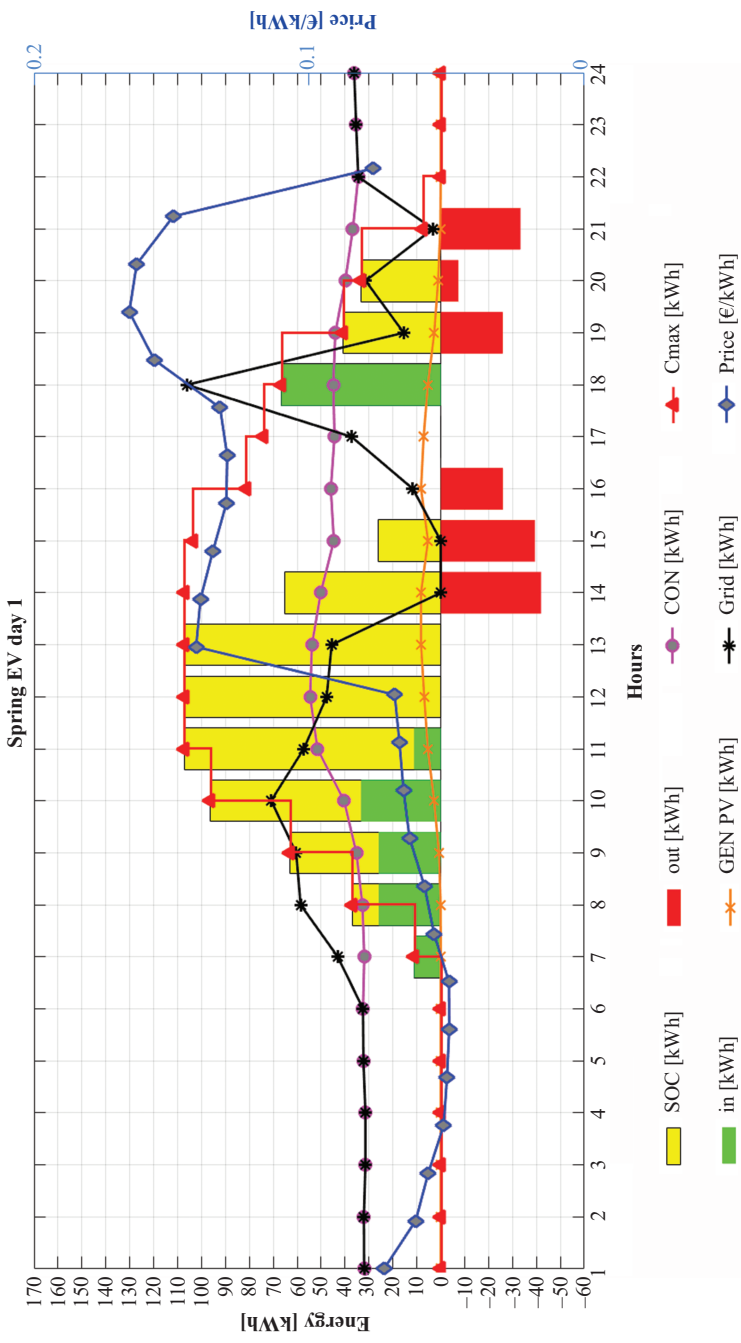


Figure 9.14 Building energy-management system behaviour day 1 (EV tariff, spring, occupation 1)

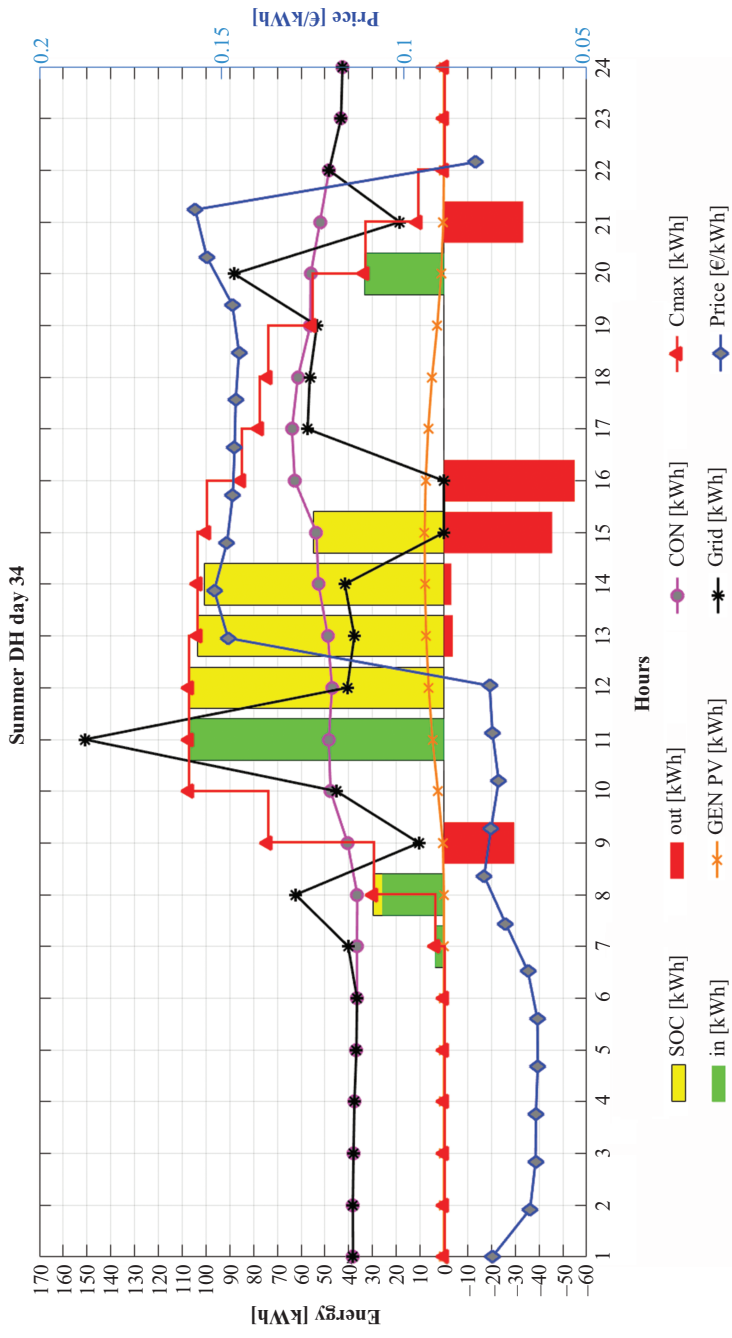


Figure 9.15 Building energy-management system behaviour day 34 (DH tariff, summer, occupation 4)

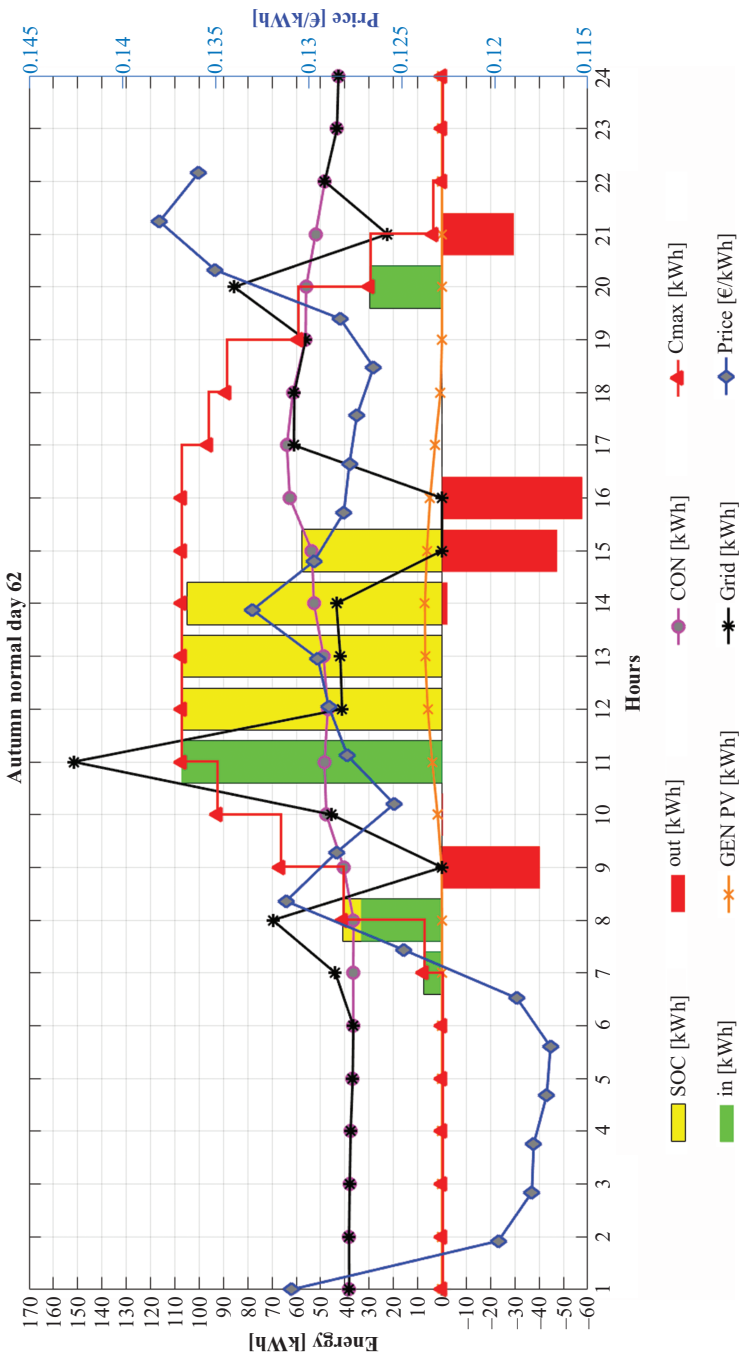


Figure 9.16 Building energy-management system behaviour day 62 (DH tariff, autumn, occupation 2)

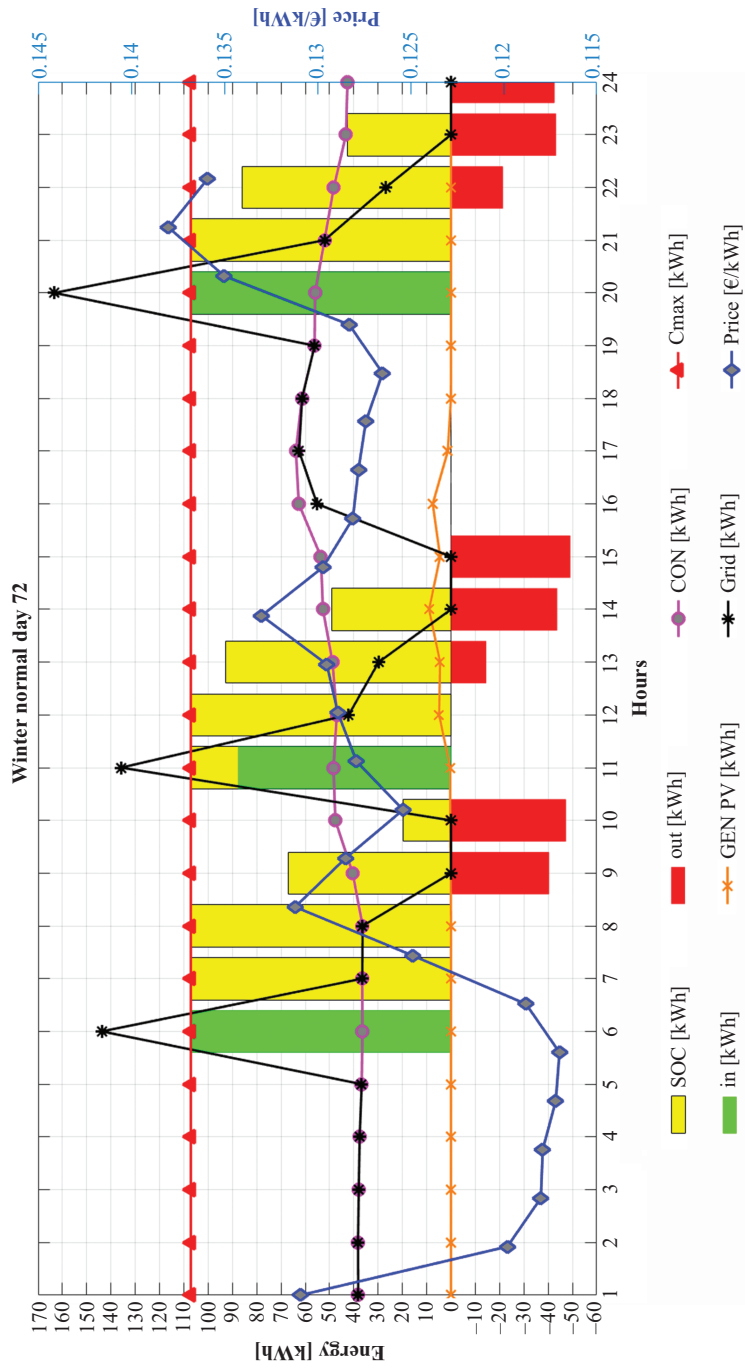


Figure 9.17 Building energy-management system behaviour day 72 (normal tariff, winter, day 72)

The next six figures show the charging/discharging profiles and the SOC evolution of the aggregated battery for the 72 different proposed scenarios.

First, Figure 9.18(a) shows the result of this optimization problem for EV tariff in the spring season (days 1 to 6). This figure presents the time evolution of the

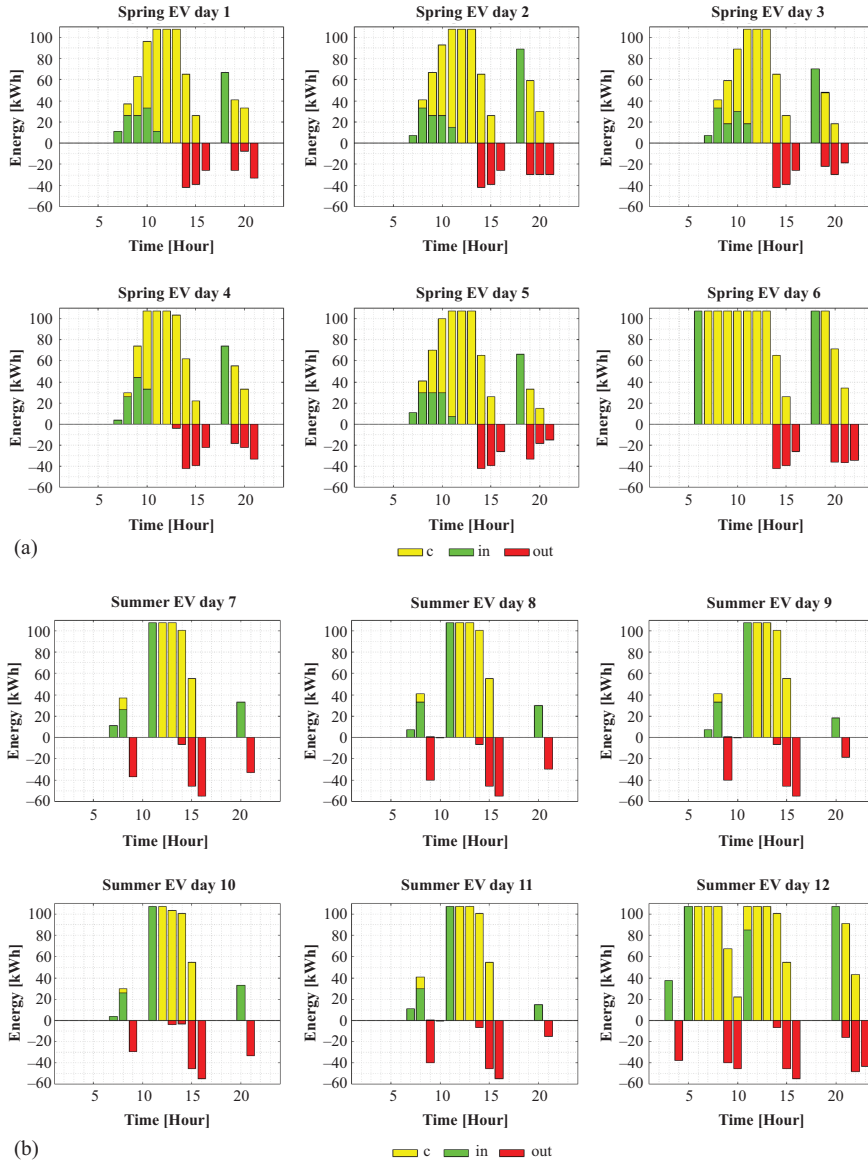


Figure 9.18 (a) SOC evolution and energy extracted/injected in the battery for days 1–6 and (b) SOC evolution and energy extracted/injected in the battery for days 7–12 (EV tariff)

aggregated battery state of charge (yellow bar), the energy extracted from the battery (red bar) and the energy injected (green bar). Figure 9.18(b) shows the same results for the summer season (days 7 to 12).

Figure 9.19(a) shows the result of this optimization problem for EV tariff in the autumn season (days 13 to 18). This figure presents the time evolution of the

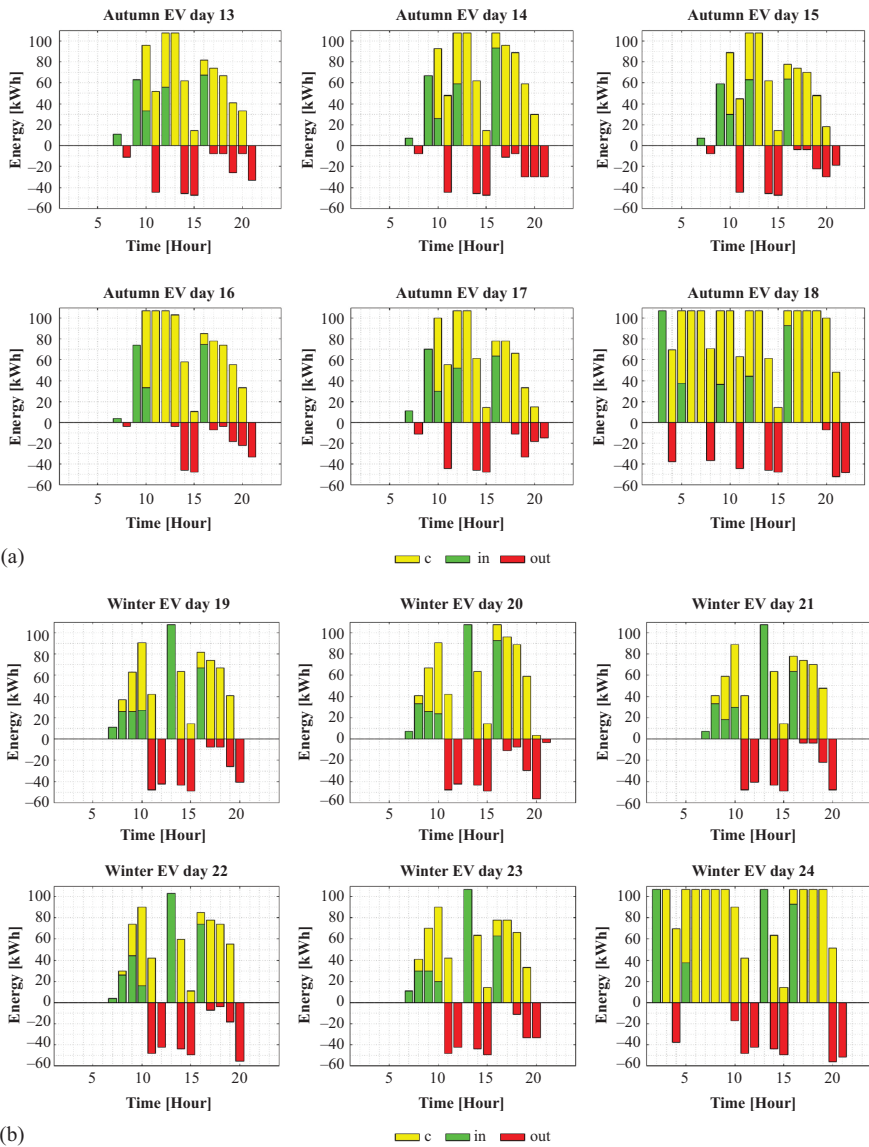


Figure 9.19 (a) SOC evolution and energy extracted/injected in the battery for days 13–18 and (b) SOC evolution and energy extracted/injected in the battery for days 19–24 (EV tariff)

aggregated battery state of charge (yellow bar), the energy extracted from the battery (red bar) and the energy injected (green bar). Figure 9.19(b) shows the same results for the winter season (days 19 to 24).

Figure 9.20(a) shows the result of this optimization problem for DH tariff in the spring season (days 25 to 30). This figure presents the time evolution of the

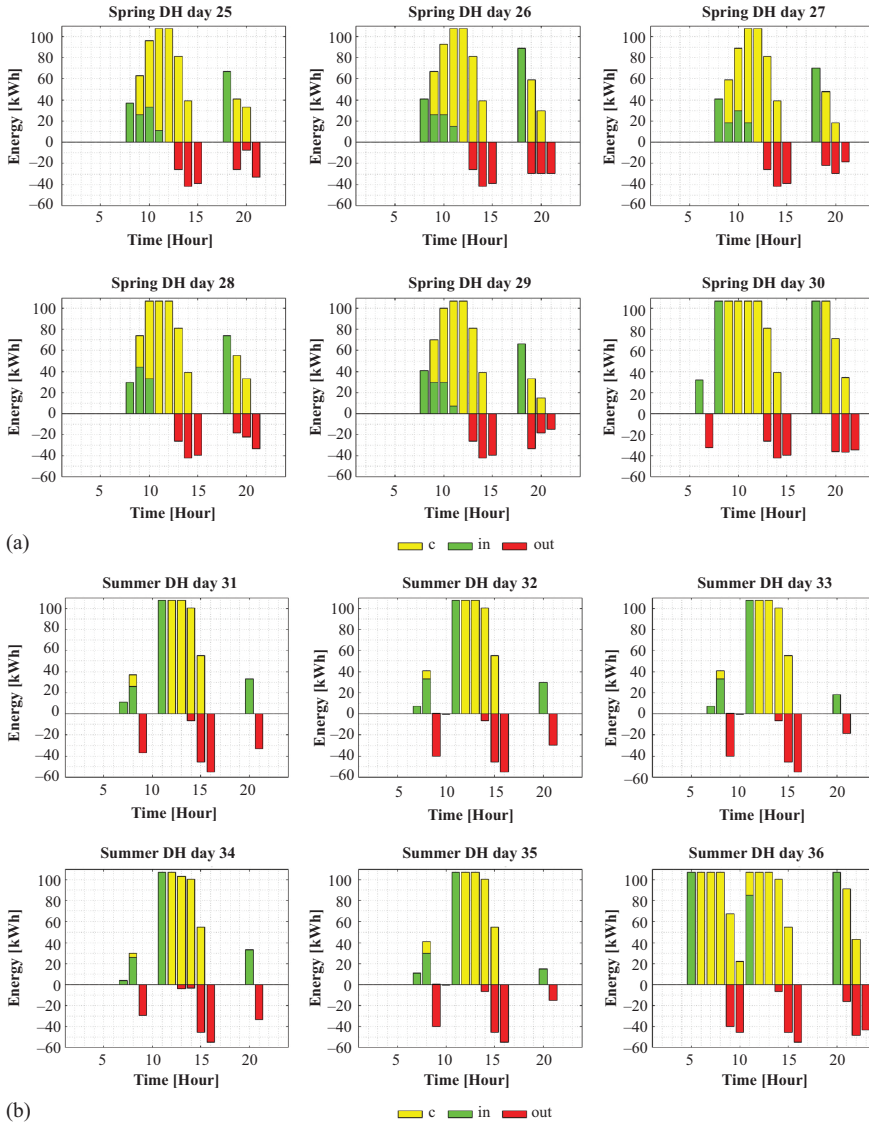


Figure 9.20 (a) SOC evolution and energy extracted/injected in the battery for days 25–30 and (b) SOC evolution and energy extracted/injected in the battery for days 31–36 (DH tariff)

aggregated battery state of charge (yellow bar), the energy extracted from the battery (red bar) and the energy injected (green bar). Figure 9.20(b) shows the same results for summer season (days 31 to 36).

Figure 9.21(a) shows the result of this optimization problem for DH tariff in the autumn season (days 37 to 42). This figure presents the time evolution of the

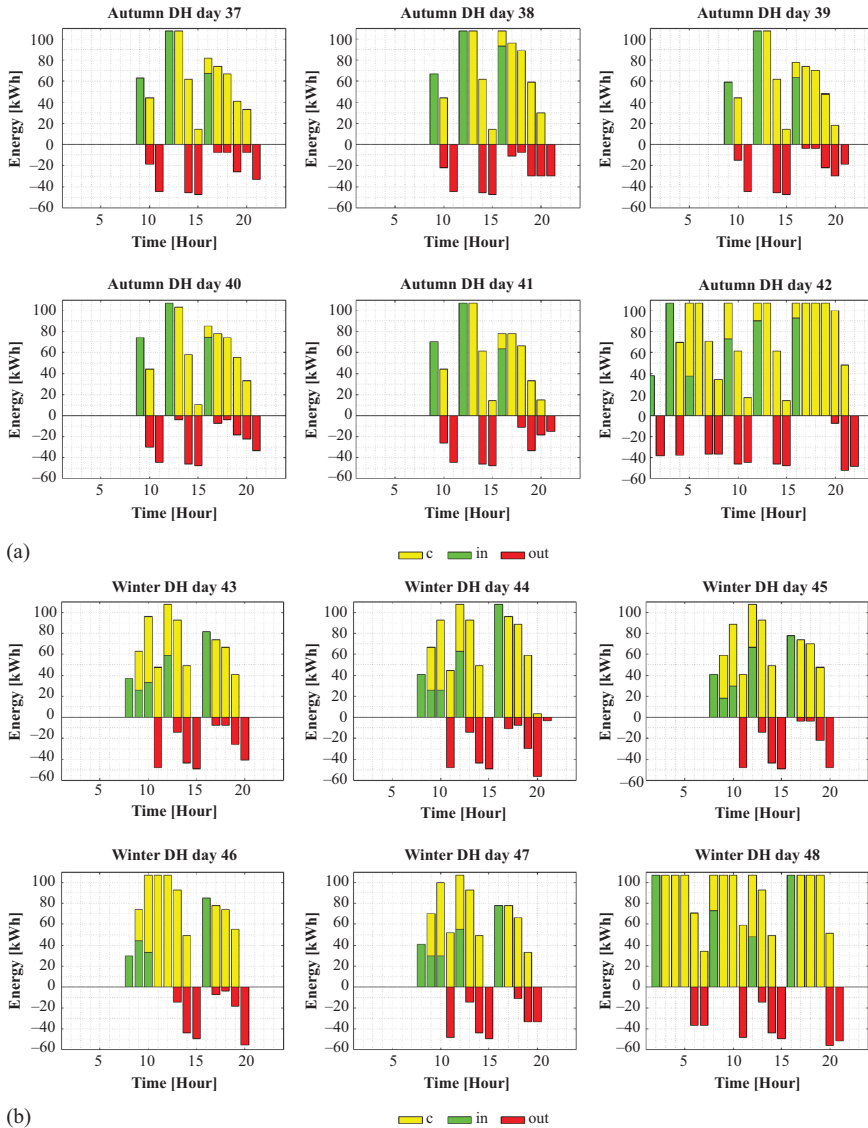


Figure 9.21 (a) SOC evolution and energy extracted/injected in the battery for days 37–42 and (b) SOC evolution and energy extracted/injected in the battery for days 43–48 (DH tariff)

aggregated battery state of charge (yellow bar), the energy extracted from the battery (red bar) and the energy injected (green bar). Figure 9.21(b) shows the same results for the winter season (days 43 to 48).

Figure 9.22(a) shows the result of this optimization problem for default normal tariff in the spring season (days 49 to 54). This figure presents the time evolution of

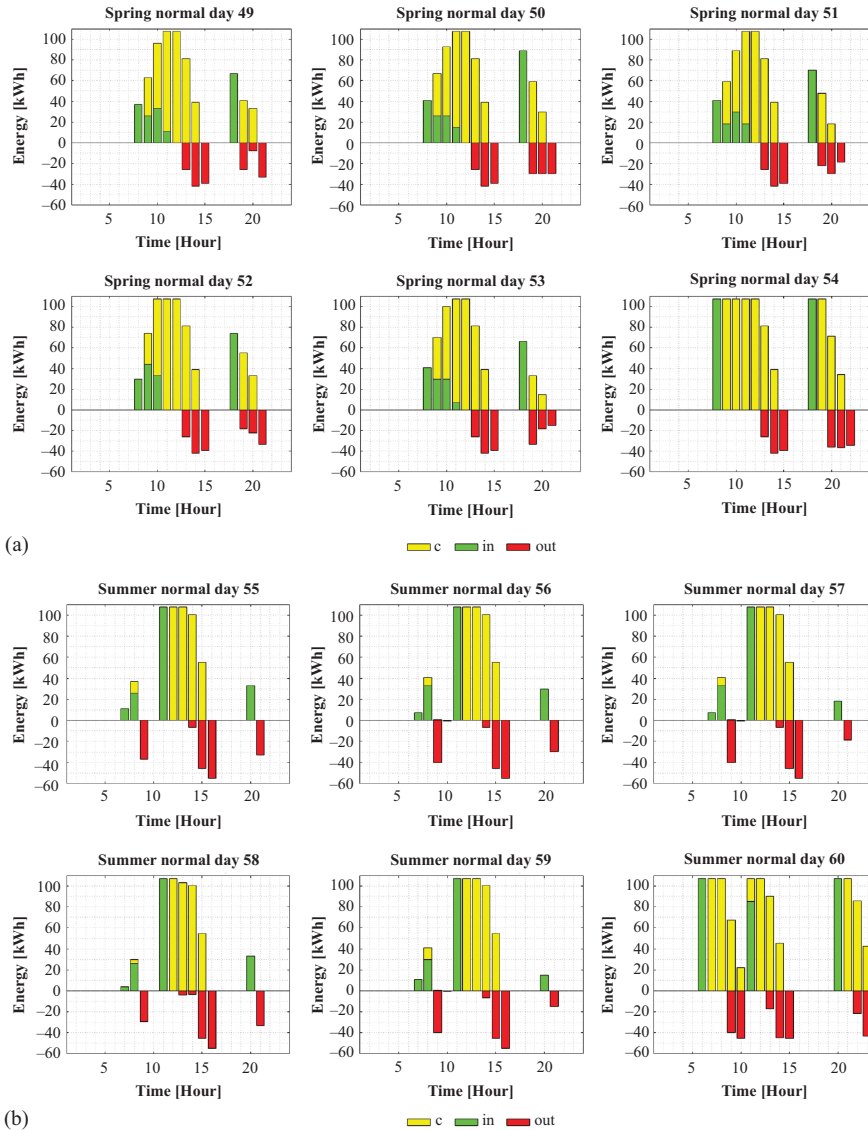


Figure 9.22 (a) SOC evolution and energy extracted/injected in the battery for days 49–54 and (b) SOC evolution and energy extracted/injected in the battery for days 55–60 (normal tariff)

the aggregated battery state of charge (yellow bar), the energy extracted from the battery (red bar) and the energy injected (green bar). Figure 9.22(b) shows the same results for the summer season (days 55 to 60).

Figure 9.23(a) shows the result of this optimization problem for default normal tariff in the autumn season (days 61 to 66). This figure presents the time evolution

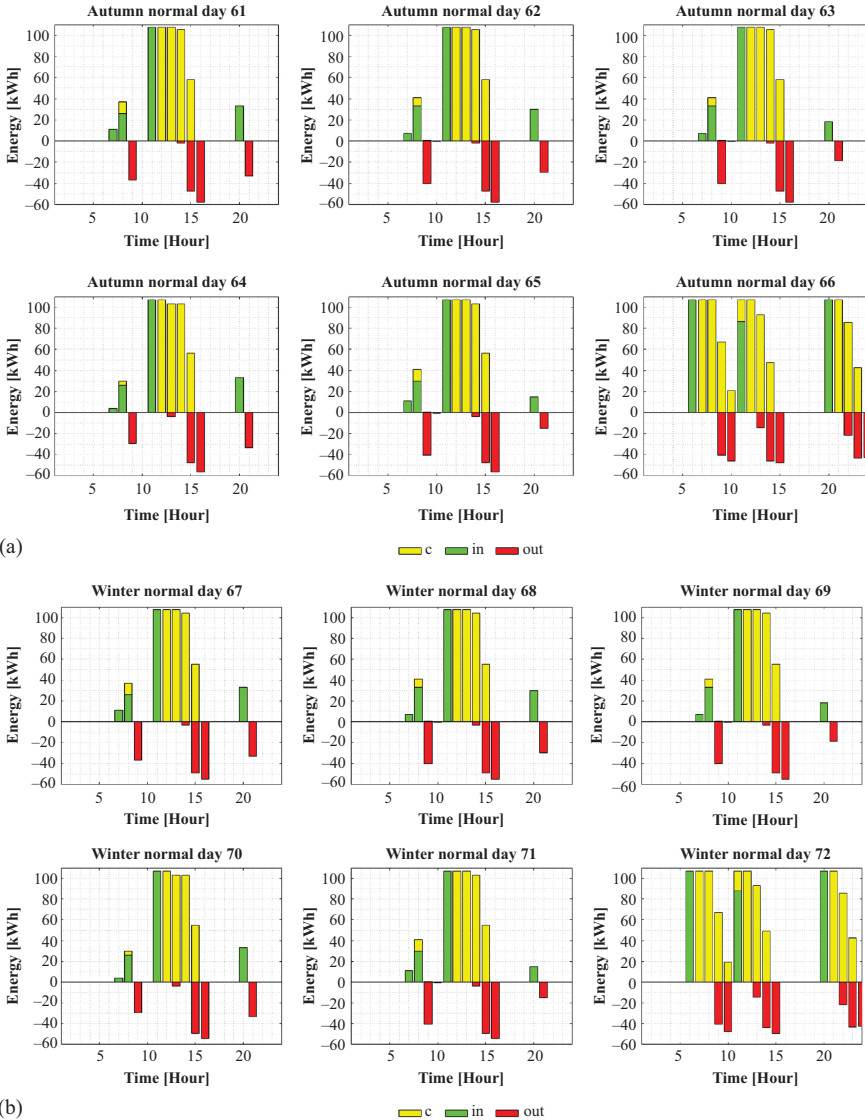


Figure 9.23 (a) SOC evolution and energy extracted/injected in the battery for days 61–66 and (b) SOC evolution and energy extracted/injected in the battery for days 66–72 (normal tariff)

of the aggregated battery state of charge (yellow bar), the energy extracted from the battery (red bar) and the energy injected (green bar). Figure 9.23(b) shows the same results for the winter season (days 67 to 72).

The total aggregated battery capacity, $c_{max}(t)$, available for this energy-management systems varies at each hour. Figure 9.24 represents these variations. Each box plot shows the minimum, 25%, median (red line), 75% and the maximum battery capacity during the day. It is important to notice that day 6 represents a constant aggregated battery capacity.

Figure 9.25 shows the aggregated battery SOC, denoted by $c(t)$, in the same scenarios. It is observed that the SOC is always lower (or equal) to the battery capacity, presented in Figure 9.24.

Table 9.3 presents the daily electricity cost for each scenario. It is observed that, if the possibility of storing energy in the aggregated battery of these EVs is not considered, the daily electricity cost paid by the building manager is constant for each season and each tariff.

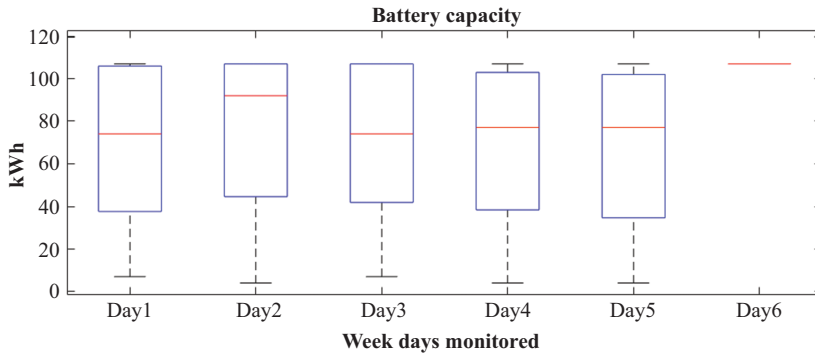


Figure 9.24 Aggregated battery capacity available under each day scenarios

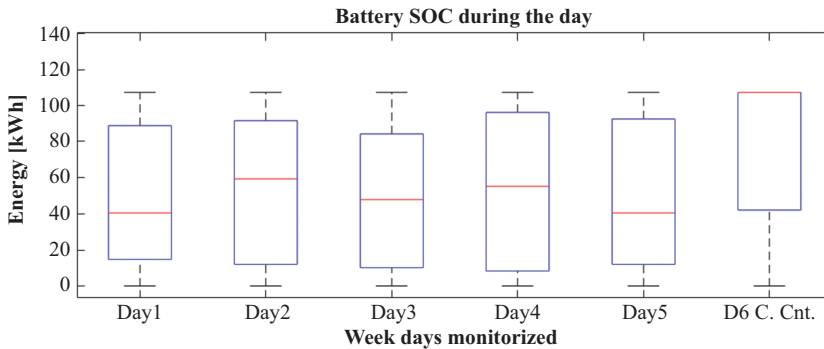


Figure 9.25 Aggregated battery SOC available under each day scenarios

Table 9.3 Electricity cost per day without (and with) the proposed optimization

Season	Payment per day [€]			Payment per day optimization [€]		
	EV tariff	DH tariff	Default tariff	EV tariff	DH tariff	Default tariff
Spring	85.77 €	85.71 €	105.17 €	75.71 €	75.22 €	102.53 €
	85.77 €	85.71 €	105.17 €	75.24 €	74.73 €	102.04 €
	85.77 €	85.71 €	105.17 €	75.70 €	75.19 €	102.50 €
	85.77 €	85.71 €	105.17 €	75.56 €	74.79 €	102.10 €
	85.77 €	85.71 €	105.17 €	75.99 €	75.51 €	102.80 €
	85.77 €	85.71 €	105.17 €	72.72 €	72.81 €	100.08 €
Summer	115.93 €	115.45 €	135.20 €	107.59 €	106.95 €	134.23 €
	115.93 €	115.45 €	135.20 €	107.62 €	106.96 €	134.24 €
	115.93 €	115.45 €	135.20 €	107.64 €	106.98 €	134.26 €
	115.93 €	115.45 €	135.20 €	107.98 €	107.30 €	134.33 €
	115.93 €	115.45 €	135.20 €	107.60 €	106.96 €	134.24 €
	115.93 €	115.45 €	135.20 €	104.96 €	104.92 €	132.25 €
Autumn	112.94 €	112.52 €	137.85 €	105.33 €	104.55 €	136.88 €
	112.94 €	112.52 €	137.85 €	105.18 €	104.38 €	136.89 €
	112.94 €	112.52 €	137.85 €	105.46 €	104.65 €	136.91 €
	112.94 €	112.52 €	137.85 €	105.53 €	104.70 €	136.97 €
	112.94 €	112.52 €	137.85 €	105.43 €	104.65 €	136.89 €
	112.94 €	112.52 €	137.85 €	102.98 €	102.74 €	134.90 €
Winter	108.42 €	107.77 €	138.86 €	99.83 €	99.25 €	137.88 €
	108.42 €	107.77 €	138.86 €	99.49 €	98.90 €	137.89 €
	108.42 €	107.77 €	138.86 €	99.80 €	99.21 €	137.91 €
	108.42 €	107.77 €	138.86 €	99.98 €	99.13 €	137.98 €
	108.42 €	107.77 €	138.86 €	99.81 €	99.23 €	137.89 €
	108.42 €	107.77 €	138.86 €	98.04 €	98.02 €	135.90 €

If the proposed OBEMS is applied, the daily electricity cost is reduced under all considered scenarios. The lowest cost is always reached under day 6 scenario, where all EVs remain parked during the day, as it were a static battery.

If the workers' mobility profiles are also considered in the optimization schedule, the occupation 2 scenario provides the lowest cost for EV tariff (during spring, autumn and winter seasons) and DH tariff (during autumn and winter seasons), while occupation 1 provides the lowest cost for the default tariff (during summer, autumn and winter seasons).

The average daily electricity cost reduction is 8.64€/day in EV tariff, 8.9€/day in DH tariff and 1.4€/day in the default tariff. The estimated annual electricity cost reduction under the proposed OBEMS varies from 2314.13€ for DH tariff (with an annual average reduction of 8.45%) to 364.52€ in the default tariff, which only represents a 1.04% of the annual electricity cost with this particular tariff.

In Figure 9.26, the average cost reduction for each tariff in each season is presented. It is observed that the highest reduction is obtained with DH tariff in spring season (with a reduction of 12.8%) and the lowest reduction is obtained with default (normal) tariff during winters.

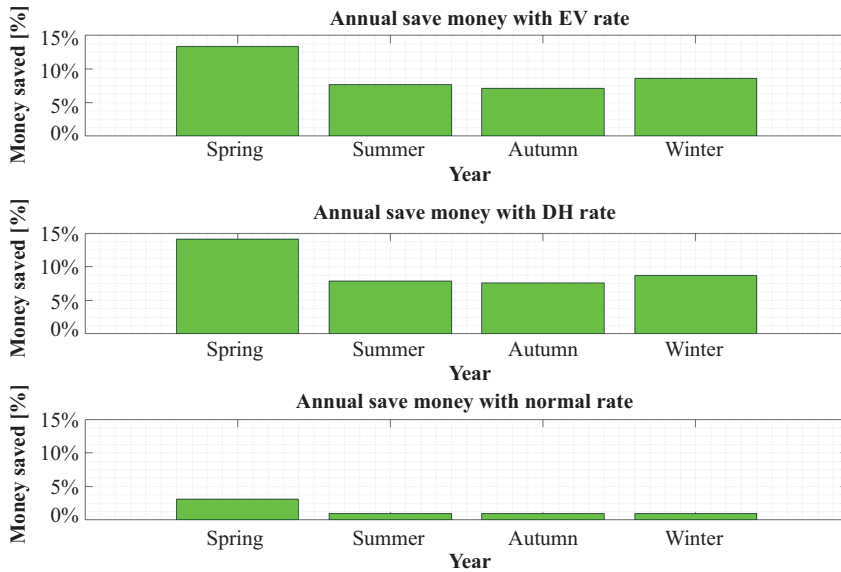


Figure 9.26 Annual saving cost for the different analysed scenarios (different seasons and different tariff)

9.5 Conclusions

The aim of this work was to analyse the integration of a parking deck with EVs with a PV system installed at a research building headquarters in Spain.

The main objective of this study was to take advantage of the distributed storage capacity available in the EVs' batteries to store surplus energy from PV systems (or during off-peak periods, when the grid electricity price is lower) and inject it back to the building electric grid after sunset or during the peak periods, when the electricity price is higher.

Seventy-two different scenarios were analysed, considering three different electricity rates, four different seasons and five different daily mobility profiles. In all studied scenarios, a cost reduction was obtained. Benefits varied mainly depending on the tariff employed. Very low benefits were obtained (less than 1.5% of cost reduction in average) when the default (normal) rate was analysed, since the difference between the maximum and minimum prices along the day is highly reduced. In this case, the investment in new infrastructure to allow this proposed optimized energy-building-management system is not justifiable. Once a larger price variation along the day is introduced with the other dual analysed tariffs (DH and EV), higher annual average cost reductions are obtained, with an average cost reduction of 8.45% in DH tariff and 8.17% in EV tariff. Additionally, DH tariff provides the lowest costs, although its difference with the EV tariff is not remarkable on a day-by-day basis (an average X%) and there are scenarios in which employing an EV tariff has a less cost than a DH tariff.

References

- [1] Marc A. Melliger, Oscar P.R. van Vliet, and Heikki Liimatainen, ‘Anxiety vs reality – Sufficiency of battery electric vehicle range in Switzerland and Finland’, *Transportation Research Part D: Transport and Environment*, Volume 65, 2018, Pages 101–115, ISSN 1361–9209, <https://doi.org/10.1016/j.trd.2018.08.011>
- [2] Katrin Seddig, Patrick Jochem, and Wolf Fichtner, ‘Integrating renewable energy sources by electric vehicle fleets under uncertainty’, *Energy*, Volume 141, 2017, Pages 2145–2153, ISSN 0360–5442, <https://doi.org/10.1016/j.energy.2017.11.140>.
- [3] Antun Pfeifer, Viktorija Dobravec, Luka Pavlinek, Goran Krajačić, and Neven Duić, ‘Integration of renewable energy and demand response technologies in interconnected energy systems’, *Energy*, Volume 161, 2018, Pages 447–455, ISSN 0360–5442, <https://doi.org/10.1016/j.energy.2018.07.134>.
- [4] International Renewable Energy Agency, IRENA, ‘Renewable Power Generation Cost in 2017’, available at: https://www.irena.org/-/media/Files/IRENA/Agency/Publication/2018/Jan/IRENA_2017_Power_Costs_2018.pdf
- [5] Nuria Martín-Chivelet, and David Montero-Gómez, ‘Optimizing photovoltaic self-consumption in office buildings’, *Energy and Buildings*, Volume 150, 2017, Pages 71–80, ISSN 0378–7788, <https://doi.org/10.1016/j.enbuild.2017.05.073>
- [6] Ghada Merei, Janina Moshövel, Dirk Magnor, and Dirk Uwe Sauer, ‘Optimization of self-consumption and techno-economic analysis of PV-battery systems in commercial applications’, *Applied Energy*, Volume 168, 2016, Pages 171–178, ISSN 0306–2619, <https://doi.org/10.1016/j.apenergy.2016.01.083>
- [7] I. Momber *et al.*, ‘Plug-in electric vehicle interactions with a small office building: An economic analysis using DER-CAM’, *IEEE PES General Meeting*, Providence, RI, 2010, Pages 1–8, doi: 10.1109/PES.2010.5589485
- [8] Claire Curry, ‘Lithium-ion battery costs and market’, *Bloomberg New Energy Finance*, 2017, available at: <https://data.bloomberglp.com/bnef/sites/14/2017/07/BNEF-Lithium-ion-battery-costs-and-market.pdf>
- [9] Red Eléctrica de España. ‘Active energy invoicing price’, available at: <https://www.esios.ree.es/en/pvpc>
- [10] Nissan USA Press Release, ‘New 2016 Nissan Leaf now offers best-in-class 107-mile range in affordable, fun-to-drive package’, available at: <http://nissannews.com/en-US/nissan/usa/releases/new-2016-nissan-leaf-now-offers-best-in-class-107-mile-range-in-affordable-fun-to-drive-package>
- [11] Spritmonitor Verbrauchswerte real erfahren, available at: <http://www.spritmonitor.de/>

